THE JOURNAL OF PHYSICAL CHEMISTRY Letters

Letter

Cite This: J. Phys. Chem. Lett. 2019, 10, 2823−2828

pubs.acs.org/JPCL

Specific Ion Effects on Hydrogen-Bond Rearrangements in the Halide−Dihydrate Complexes

Pushp Bajaj,*[,†] Debbie Zhuang,[†] and Francesco Paesani*[,†,‡,§]

[†]Department of Chemistry and Biochemistry, University of California, San Diego, La Jolla, California 92093, United States

[‡]Materials Science and Engineering, University of California, San Diego, La Jolla, California 92093, United States

[§]San Diego Supercomputer Center, University of California, San Diego, La Jolla, California 92093, United States

Supporting Information

ABSTRACT: Small aqueous ionic clusters represent ideal systems to investigate the microscopic hydrogen-bonding structure and dynamics in ion hydration shells. In this context, halide−dihydrate complexes are the smallest systems where the interplay between halide−water and water−water interactions can be studied simultaneously. Here, quantum molecular dynamics simulations unravel specific ion effects on the temperature-dependent structural transition in $X^-(H_2O)_2$ complexes (X = Cl, Br, and I), which is induced by the breaking of the water−water hydrogen bond. A systematic analysis of the hydrogen-bonding rearrangements at low temperature provides fundamental insights into the competition between halide−water and water−water interactions depending on the properties of the halide ion. While the halide−water hydrogen-bond strength decreases going from $Cl^-(H_2O)_2$ to $I^-(H_2O)_2$, the opposite trend in observed in the strength of the water−water hydrogen-bond, suggesting that nontrivial many-body effects may also be at play in the hydration shells of halide ions in solution, especially in frustrated systems (e.g., interfaces) where the water molecules can have dangling OH bonds.

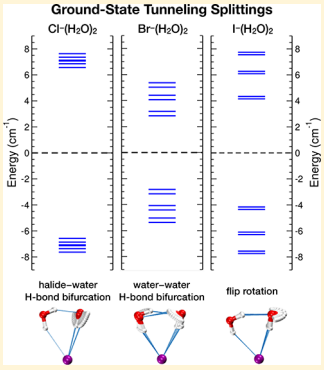

Ionic aqueous systems are ubiquitous. For example, they exist inside living cells[1−6] and in the environment[7−9] and are central components of many devices, including electrolytic cells, capacitors, and batteries.[10] An accurate characterization of the underlying interactions between the ions and the surrounding water molecules is central for understanding specific ion effects as well as for controlling the underlying physicochemical processes. While there have been extensive experimental and computational studies on ion hydration,[8,11−17] a definitive picture of how the ions are hydrated and to what extent structural differences in the organization of the hydration shells translate into differences in the thermodynamic and dynamical properties of the corresponding ionic systems is still lacking.

Ion−water clusters are ideal systems to validate the ability of molecular models to characterize the molecular mechanisms associated with hydrogen-bonding (H-bonding) rearrangements, since, due to their relatively small sizes, they are amenable to high-level molecular modeling[12,18−36] and, at the same time, can be studied experimentally using high-resolution vibrational spectroscopy.[37−40] In this context, halide dihydrates hold a special place since they are the smallest complexes in which two water molecules can be simultaneously H-bonded to each other and to the ion, thus allowing for directly probing the interplay between ion−water and water−water interactions.

Building upon our recent study of isotope effects and tunneling in the isotopomers of the $I^-(H_2O)_2$ complex,[34] we report here a systematic analysis of the structure and temperature-dependent evolution of the $X^-(H_2O)_2$ dihydrates (with X = Cl, Br, and I), which provides fundamental insights into how halide ions with different sizes, charge densities, and polarizabilities affect the H-bond rearrangement dynamics within similar complexes. Anharmonic vibrational frequency calculations and path integral molecular dynamics (PIMD) simulations performed for all three halide−dihydrates using the halide−water MB-nrg many-body potential energy functions (PEFs) introduced in refs 32 and 33 predict a transition from *closed* cyclic arrangements, where the two water molecules are H-bonded to the halide ion and to each other, to *open* arrangements, where the water−water H-bond is broken. At low temperature, when the complexes exist predominantly in the *closed* configuration, ring-polymer instanton (RPI) calculations provide unambiguous evidence for H-bond rearrangements taking place in all three halide−dihydrates via quantum tunneling mediated by the presence of the halide ion.

To provide context for our analysis, anharmonic vibrational frequencies calculated for the global minimum energy configurations of all three $X^-(H_2O)_2$ dihydrates (Figure 1a) using the combined local-mode[41,42] and local-monomer[43] methods (see Supporting Information for details) are compared in Figure 1b with the corresponding values measured in argon tagged-vibrational predissociation experi-

Received: March 29, 2019
Accepted: May 13, 2019
Published: May 13, 2019

DOI: 10.1021/acs.jpclett.9b00899
J. Phys. Chem. Lett. 2019, 10, 2823−2828

a)

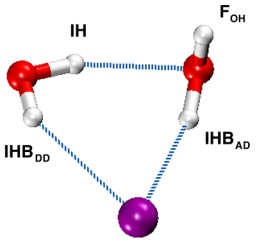

b)

Mode	$Cl^-(H_2O)_2$		$Br^-(H_2O)_2$		$I^-(H_2O)_2$	
	Theory	Experiment	Theory	Experiment	Theory	Experiment
2HOH bend	3211/3265	3202/3301	3174/3254	3267/3290	3178/3238	3237
IHB_{AD}	3085	3130	3233	3207	3337	3344
IHB_{DD}	3363	3375	3430	3438	3500	3504/3516
IH	3619	3633	3609	3625	3594	3619
F_{OH}	3692	3686	3690	3680	3684	3684

Figure 1. (a) Schematic representation of the global minimum energy configuration of the three halide−dihydrate complexes analyzed in this study. (b) OH-stretch vibrational frequencies (in cm^{-1}) for the $Cl^-(H_2O)_2$, $Br^-(H_2O)_2$, and $I^-(H_2O)_2$ complexes. Experimental values for the $Cl^-(H_2O)_2$ and $Br^-(H_2O)_2$ clusters are taken from ref 23 while those for the $I^-(H_2O)_2$ complex are taken from ref 38.

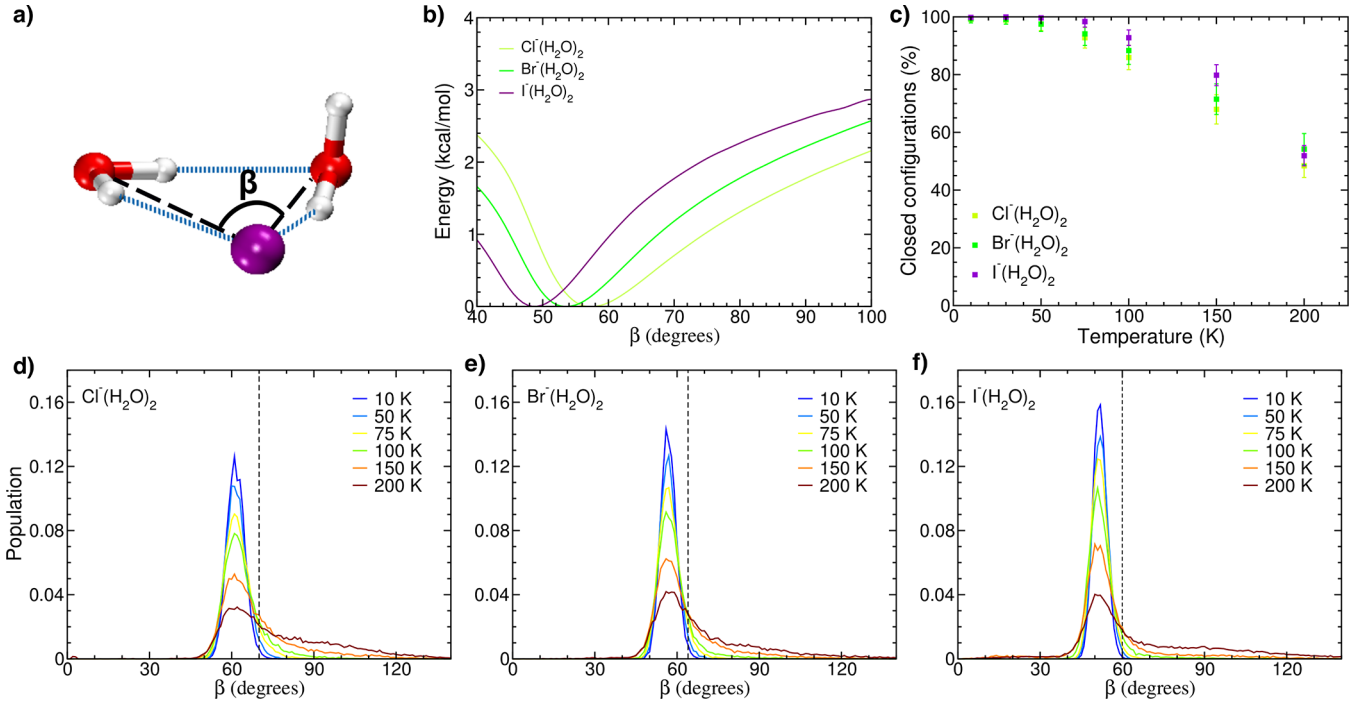

Figure 2. (a) Schematic representation of the O−X−O′ (β) angle used to classify *closed* and *open* configurations. (b) One-dimensional potential energy scans along the β angle. (c) Relative populations of *closed* configurations calculated from PIMD simulations carried out as a function of temperature for the $Cl^-(H_2O)_2$, $Br^-(H_2O)_2$, and $I^-(H_2O)_2$ complexes. (d)−(f) Normalized probability distributions of the β angle calculated from PIMD simulations carried out as a function of temperature for the $Cl^-(H_2O)_2$, $Br^-(H_2O)_2$, and $I^-(H_2O)_2$ complexes, respectively.

ments.[23,38] The minimum energy configuration of each $X^-(H_2O)_2$ complex exhibits a cyclic arrangement where the two water molecules form H-bonds to the halide ion and a single H-bond to each other. Based on the H-bonding environment within the complex, the two water molecules are classified as donor−donor (DD), donating two H-bonds, and acceptor−donor (AD), accepting one H-bond and donating one H-bond, respectively. As a consequence, the four OH-bonds, labeled as IHB_{DD}, IHB_{AD}, IH, and F_{OH}, are associated with four distinct vibrational frequencies (Figure 1). For all three $X^-(H_2O)_2$ complexes, the calculated anharmonic frequencies are in excellent agreement with the corresponding experimental values, providing further evidence for the accuracy of the MB-nrg PEFs.[32,33] Clearly, the IHB_{DD} and IHB_{AD} vibrational frequencies, corresponding to the two H-bonded-to-halide positions, increase going from chloride to iodide as the halide−water H-bond strength decreases. However, there is a slight decrease in the IH vibrational frequency corresponding to the H-bonded-to-water position, suggesting an increase in the water−water H-bond strength going from $Cl^-(H_2O)_2$ to $I^-(H_2O)_2$. These findings are in agreement with previous studies assessing the trends in the halide−water and water−water interactions in small halide−water clusters, which suggest that the presence of the halide ion weakens the water−water H-bond strength.[12,23−25,44]

The variation of the water−water H-bond strength in the $X^-(H_2O)_2$ complexes can be further quantified through the analysis of one-dimensional potential energy scans along the

DOI: 10.1021/acs.jpclett.9b00899
J. Phys. Chem. Lett. 2019, 10, 2823−2828

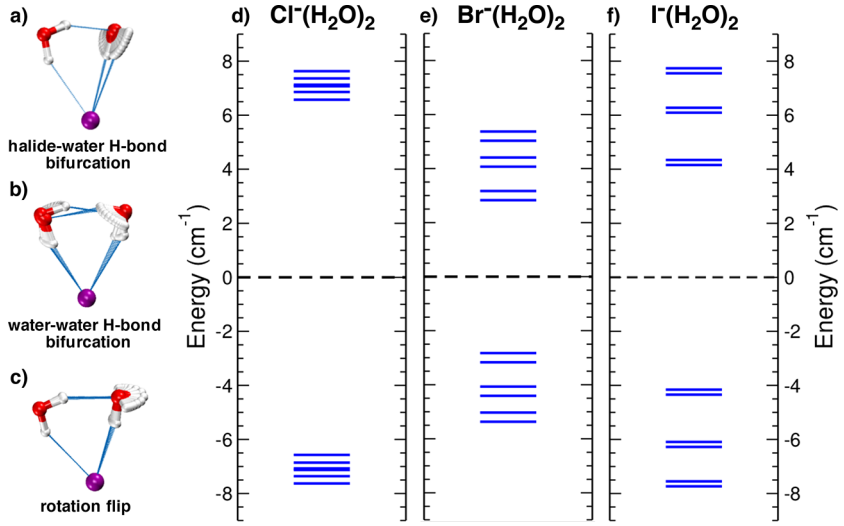

Figure 3. (a)−(c) Schematic representations of the halide−water H-bond bifurcation, water−water H-bond bifurcation, and flip rotation pathways, respectively, in the $X^-(H_2O)_2$ complexes. (d)−(f) Ground-state tunneling splitting patterns for the $Cl^-(H_2O)_2$, $Br^-(H_2O)_2$, and $I^-(H_2O)_2$ complexes, respectively. See main text for details.

O−X−O′ angle (denoted as β in Figure 2a) characterizing the transition from *closed* to *open* configurations. As shown in Figure 2b, each of the three potential energy scans exhibits a minimum value for β corresponding to the *closed* configuration with an intact water−water H-bond and then plateaus for larger values of β as the water−water H-bond breaks. The energy required to break the water−water H-bond is the smallest for the $Cl^-(H_2O)_2$ complex which, consequently, is characterized by the weakest water−water H-bond among the three halide−dihydrates.

In order to characterize the structural evolution of all three complexes as a function of temperature, normalized probability distributions of the β angle computed from PIMD simulations are shown in Figure 2d−f for $Cl^-(H_2O)_2$, $Br^-(H_2O)_2$, and $I^-(H_2O)_2$, respectively. At low temperature, all three distributions are spread over narrow ranges of β, where the complexes exist exclusively in *closed* configurations. As the temperature increases, a shoulder starts to appear for larger values of β, indicating that the water−water H-bond start breaking and the complex transitions to the *open* configuration. This transition can be easily quantified by classifying the instantaneous molecular configurations as *closed* or *open* using a cutoff value for β and calculating the relative populations of both types of configurations as a function of temperature (Figure 2c). A cutoff value of $\beta = 70 \pm 2°$, $64 \pm 2°$, and $60 \pm 2°$ was chosen for the $Cl^-(H_2O)_2$, $Br^-(H_2O)_2$, and $I^-(H_2O)_2$ complexes, respectively, to classify the configurations as *closed*. Since the water−water H-bond strength increases going from $Cl^-(H_2O)_2$ to $I^-(H_2O)_2$, the water−water H-bond starts to break at a lower temperature (∼75 K) in the chloride−dihydrate complex and at a higher temperature (∼100 K) in both bromide− and iodide−dihydrate complexes. As entropic contributions become dominant at higher temperature, the small energy differences between the three halide−dihydrates are diminished and the corresponding distributions overlap.

While the large-amplitude fluctuations leading to breaking of the water−water H-bond can be probed through experimental vibrational spectroscopy, the faster water rotational motions leading to H-bond rearrangements within each complex cannot be detected using current experimental setups. As first reported for the iodide−dihydrate complex in ref 34, our simulations indicate that, below ∼50 K, when all three halide−dihydrate complexes exist in *closed* configurations characterized by four distinct H positions (Figure 1a), the H atoms can exchange their positions through rotational tunneling pathways. Specifically, three feasible quantum tunneling pathways (Figure 3a−c), corresponding to the halide−water H-bond bifurcation, water−water H-bond bifurcation, and flip rotation, are identified from the RPI simulations (see the Supporting Information for details).[34,45,46] The first two pathways involve the breaking and forming of a single H-bond, while the third pathway involves a simple out-of-plane rotation of the free OH-bond of the AD water molecule. The individual tunneling splitting values associated with the three pathways for each halide−dihydrate are listed in Table 1. Since the coupling between the three pathways gives rise to a complicated tunneling splitting pattern of the otherwise degenerate ground state, the energy splitting patterns for all three halide−dihydrate complexes shown in Figure 3d−f are obtained from the diagonalization of the corresponding tunneling Hamiltonian matrices.[34,46]

Table 1. Tunneling Matrix Elements, $-h$, in cm^{-1}, for the $Cl^-(H_2O)_2$, $Br^-(H_2O)_2$, and $I^-(H_2O)_2$ Clusters

	$Cl^-(H_2O)_2$	$Br^-(H_2O)_2$	$I^-(H_2O)_2$
halide−water H-bond bifurcation	0.29	1.1	5.9
water−water H-bond bifurcation	7.1	4.1	1.7
flip rotation	0.25	0.17	0.09

The individual tunneling splittings associated with the three pathways and, consequently, the overall ground-state tunneling splitting patterns are significantly different among the three halide−dihydrates. The changes in the individual tunneling splitting values, particularly those corresponding to the two H-bond bifurcation pathways, can be attributed to changes in the relative strength of the halide−water and water−water interactions. Since the tunneling splitting values depend directly on the height and shape of the potential energy barrier along the corresponding tunneling pathways and the halide−water H-bond strength decreases significantly from chloride−water to iodide−water, the tunneling splitting value

DOI: 10.1021/acs.jpclett.9b00899
J. Phys. Chem. Lett. 2019, 10, 2823−2828

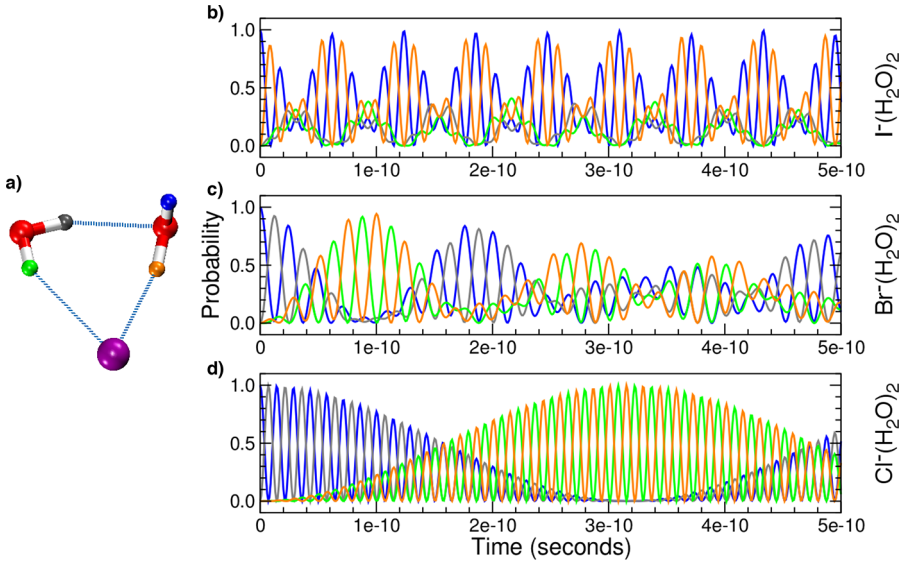

Figure 4. Time evolution of the probabilities of each of the four positions of the hydrogen atom in the $I^-(H_2O)_2$ (b), $Br^-(H_2O)_2$ (c), and $Cl^-(H_2O)_2$ (d) clusters, starting from the free OH position indicated in blue (see text for details). The colors of the four curves correspond to the four different positions of the hydrogen atom (a).

associated with the halide−water H-bond bifurcation pathway increases by more than a factor of 10 from $Cl^-(H_2O)_2$ to $I^-(H_2O)_2$, as shown in Table 1. The opposite trend is observed for the water−water tunneling splitting value since the barrier height along the water−water H-bond bifurcation pathway slightly increases going from $Cl^-(H_2O)_2$ to $I^-(H_2O)_2$ (see the Supporting Information for details). Following the same argument, the decreasing trend in the tunneling matrix element associated with the flip rotation pathway can be explained by the increasing trend in the barrier height corresponding to this pathway, i.e., 0.85 kcal/mol for $Cl^-(H_2O)_2$, 0.98 kcal/mol for $Br^-(H_2O)_2$, and 1.12 kcal/mol for $I^-(H_2O)_2$.

As mentioned above, current vibrational spectroscopy techniques for ionic clusters do not have high enough resolution to detect such small energy level splittings as predicted by the present RPI simulations. Hence, the time scales associated with the individual tunneling pathways shown in Figure 3a−c could provide a useful measure to guide comparisons between theory and future experiments. Following the same procedure as described in ref 34, tunneling time scales for exchange between the four H positions through the H-bond bifurcation pathways are calculated by monitoring the evolution of the H-bonding arrangements in each complex through the propagation of the time-dependent Schrödinger equation under the action of the tunneling Hamiltonian. Figure 4b−d shows the probabilities for a H atom initially (t = 0) located in the free position (blue H atom in Figure 4a) of the $Cl^-(H_2O)_2$, $Br^-(H_2O)_2$, and $I^-(H_2O)_2$ complexes to be found in any of the four different positions at a later time t. As a direct consequence of the differences in the tunneling splitting values listed in Table 1, the exchange between the blue and orange H positions (Figure 4a), which takes place through the halide−water H-bond bifurcation pathway, is found to be the slowest for the chloride−dihydrate and becomes progressively faster in $Br^-(H_2O)_2$ and $I^-(H_2O)_2$. The opposite trend is found for the exchange between the blue and gray H positions (Figure 4a), which takes place through the water−water H-bond bifurcation pathway. In this case, the tunneling motion is the fastest for the chloride−dihydrate and becomes progressively slower in $Br^-(H_2O)_2$ and $I^-(H_2O)_2$. Additional analyses of the temperature-dependent free-energy profiles associated with the three pathways are provided in the Supporting Information.

By combining accurate many-body representations of halide−water and water−water interactions with state-of-the-art quantum dynamics simulations, this study provides a comprehensive analysis of the structure, H-bond rearrangements, and temperature-dependent evolution of the $X^-(H_2O)_2$ complexes, with X = Cl, Br, and I. At low temperature, the complexes exist in the global minimum energy (cyclic) configuration with the two water molecules simultaneously H-bonded to the halide ion and to each other. In this configuration, the four OH-bonds experience significantly different H-bonding environments, which results in four distinct peaks in the corresponding vibrational spectra. Rotational tunneling pathways (as introduced in ref 34 for the iodide−dihydrate complex) were identified, which result in complete scrambling of the four OH-bonds in all three halide−dihydrate complexes, leading to well-defined tunneling splitting patterns that were calculated using RPI simulations. At a higher temperature (above ∼75 K) the complexes partially "dissociate" as the water−water H-bond breaks and the complexes transition to *open* configurations with the two water molecules being only H-bonded to the halide ion. This transition is associated with major changes in the vibrational spectra, as shown previously in temperature-dependent experiments carried out for $I^-(H_2O)_2$.[37] Although temperature-dependent measurements are currently not available for $Cl^-(H_2O)_2$ and $Br^-(H_2O)_2$, our analysis suggests that similar progressions of the spectral features as a function of temperature should be expected for these complexes as well.

For the low-temperature *closed* configurations, the vibrational spectra and tunneling splitting values associated with the halide−water H-bond bifurcation pathway show a clear trend mirroring the decreasing strength of halide−water interactions going from the chloride−dihydrate to the iodide−dihydrate. This leads to significantly different H-bond rearrangement

DOI: 10.1021/acs.jpclett.9b00899
J. Phys. Chem. Lett. 2019, 10, 2823−2828

dynamics among the three $X^-(H_2O)_2$ complexes. As the halide−water H-bond strength decreases, going from $Cl^-(H_2O)_2$ to $I^-(H_2O)_2$, the water−water H-bond strength slightly increases, which is most evident from the decrease in the tunneling splitting values associated with the water−water H-bond bifurcation pathway. This can also be seen in the temperature-dependent evolution of the complexes, with the temperature at which the water−water H-bond starts to break increasing from $Cl^-(H_2O)_2$ to $I^-(H_2O)_2$.

Previous studies have established that tunneling pathways leading to H-bond rearrangements exist in the water dimer and trimer[46] as well as halide−monohydrates.[29,31,33] Building upon the results of ref 34, the present study provides further evidence for quantum tunneling pathways in halide−dihydrates along with a comprehensive analysis of the temperature-dependent H-bond rearrangement dynamics. Since the water trimer in its minimum energy configuration has a cyclic arrangement similar to that of the three halide−dihydrates studied here, it is thus not surprising that similar flip rotation and water−water H-bond bifurcation tunneling pathways exist in both complexes. Compared to the water trimer, the present results demonstrate that the halide ion drastically weakens the water−water H-bond, leading to significantly faster tunneling dynamics. Importantly, the flip rotation, which is the fastest motion in the water trimer, becomes the slowest in the halide−dihydrate complexes. As originally noted in ref 34, this difference is explained by considering the relatively higher energy barrier associated with the flip rotation pathway (0.85 kcal/mol for $Cl^-(H_2O)_2$, 0.98 kcal/mol for $Br^-(H_2O)_2$, and 1.12 kcal/mol for $I^-(H_2O)_2$) in the halide−dihydrates compared to that in the water trimer (0.47 kcal/mol).[46]

While our results indicate that the presence of halide ions in the halide−dihydrate complexes speeds up the H-bond rearrangement dynamics compared to the pure water trimer, ultrafast vibrational spectroscopy measurements of salt solutions suggest that the H-bond dynamics within the first hydration shell of the halide ions is significantly slowed down compared to that of pure water.[47−49] As previously noted,[34] the H-bonding environments in the halide−dihydrates are significantly different from those found in solution. In particular, the halide−dihydrates are characterized by a free OH-bond, which triggers the overall H-bond rearrangement within the complexes, thus leading to faster water reorientation along both halide−water and water−water H-bond bifurcation pathways. Our analysis of halide−dihydrates thus raises the question whether faster H-bond dynamics in the first hydration shell of halide ions may be observed in frustrated systems, such as interfaces, where water molecules H-bonded to the ion can be undercoordinated, with at least one dangling OH-bond. In addition, the present quantum simulations of the H-bond dynamics in halide−dihydrates provide indirect evidence for the importance of many-body effects in water H-bond rearrangements around halide ions in solution, which, involving water molecules beyond the first hydration shell, may lead to a slowdown of the overall dynamics, reversing the trend observed in the gas phase.

■ ASSOCIATED CONTENT

Supporting Information

The Supporting Information is available free of charge on the ACS Publications website at DOI: 10.1021/acs.jpclett.9b00899.

Theoretical methods and simulation details and quantum free energies and hydrogen-bond rearrangement pathways (including quantum PMFs, tunneling matrix elements, tunneling splitting patterns) (PDF)

■ AUTHOR INFORMATION

Corresponding Authors

*E-mail: pbajaj@ucsd.edu.

*E-mail: fpaesani@ucsd.edu.

ORCID

Francesco Paesani: 0000-0002-4451-1203

Notes

The authors declare no competing financial interest.

■ ACKNOWLEDGMENTS

We thank Jeremy O. Richardson for helping with the tunneling splitting calculations of the $X^-(H_2O)_2$ complexes using the ring-polymer instanton (RPI) method. This research was supported by the National Science Foundation Center through grants nos. CHE-1305427 and CHE-1453204. Calculations were performed using the Extreme Science and Engineering Discovery Environment (XSEDE), which is supported by the National Science Foundation (grant no. ACI-1053575, allocation TG-CHE110009), the High Performance Computing Modernization Program (HPCMP) through grant no. FA9550-16-1-0327 from the Air Force Office of Scientific Research, and the Triton Shared Computing Cluster (TSCC) at the San Diego Supercomputer Center (SDSC).

■ REFERENCES

(1) Nahar, S.; Tajmir-Riahi, H. Do Metal Ions Alter the Protein Secondary Structure of a Light-Harvesting Complex of Thylakoid Membranes? *J. Inorg. Biochem.* **1995**, *58*, 223−234.

(2) Woodson, S. A. Metal Ions and RNA Folding: a Highly Charged Topic with a Dynamic Future. *Curr. Opin. Chem. Biol.* **2005**, *9*, 104−109.

(3) Draper, D. E. RNA Folding: Thermodynamic and Molecular Descriptions of the Roles of Ions. *Biophys. J.* **2008**, *95*, 5489−5495.

(4) Collins, K. D.; Neilson, G. W.; Enderby, J. E. Ions in Water: Characterizing the Forces that Control Chemical Processes and Biological Structure. *Biophys. Chem.* **2007**, *128*, 95−104.

(5) Kunz, W. Specific Ion Effects in Colloidal and Biological Systems. *Curr. Opin. Colloid Interface Sci.* **2010**, *15*, 34−39.

(6) Lo Nostro, P.; Ninham, B. W. Hofmeister Phenomena: An Update on Ion Specificity in Biology. *Chem. Rev.* **2012**, *112*, 2286−2322.

(7) Harrison, R. G.; Tammet, H. Ions in the Terrestrial Atmosphere and Other Solar System Atmospheres. *Space Sci. Rev.* **2008**, *137*, 107−118.

(8) Tobias, D. J.; Stern, A. C.; Baer, M. D.; Levin, Y.; Mundy, C. J. Simulation and Theory of Ions at Atmospherically Relevant Aqueous Liquid-Air Interfaces. *Annu. Rev. Phys. Chem.* **2013**, *64*, 339−359.

(9) Lehtipalo, K.; Rondo, L.; Kontkanen, J.; Schobesberger, S.; Jokinen, T.; Sarnela, N.; Kürten, A.; Ehrhart, S.; Franchin, A.; Nieminen, T.; et al. The Effect of Acid−Base Clustering and Ions on the Growth of Atmospheric Nano-Particles. *Nat. Commun.* **2016**, *7*, 11594.

(10) Winter, M.; Brodd, R. J. What Are Batteries, Fuel Cells, and Supercapacitors? *Chem. Rev.* **2004**, *104*, 4245−4270.

(11) Elrod, M. J.; Saykally, R. J. Many-Body Effects in Intermolecular Forces. *Chem. Rev.* **1994**, *94*, 1975−1997.

(12) Robertson, W. H.; Johnson, M. A. Molecular Aspects of Halide Ion Hydration: The Cluster Approach. *Annu. Rev. Phys. Chem.* **2003**, *54*, 173−213.

DOI: 10.1021/acs.jpclett.9b00899
J. Phys. Chem. Lett. 2019, 10, 2823−2828

(13) Jungwirth, P.; Tobias, D. J. Specific Ion Effects at the Air/Water Interface. *Chem. Rev.* **2006**, *106*, 1259−1281.
(14) Marcus, Y. Effect on Ions on the Structure of Water: Structure Making and Breaking. *Chem. Rev.* **2009**, *109*, 1346−1370.
(15) Heine, N.; Asmis, K. R. Cryogenic Ion Trap Vibrational Spectroscopy of Hydrogen-Bonded Clusters Relevant to Atmospheric Chemistry. *Int. Rev. Phys. Chem.* **2015**, *34*, 1−34.
(16) Cisneros, G. A.; Wikfeldt, K. T.; Ojamäe, L.; Lu, J.; Xu, Y.; Torabifard, H.; Bartók, A. P.; Csányi, G.; Molinero, V.; Paesani, F. Modeling Molecular Interactions in Water: From Pairwise to Many-Body Potential Energy Functions. *Chem. Rev.* **2016**, *116*, 7501−7528.
(17) Bakker, H. J.; Skinner, J. L. Vibrational Spectroscopy as a Probe of Structure and Dynamics in Liquid Water. *Chem. Rev.* **2010**, *110*, 1498.
(18) Combariza, J. E.; Kestner, N. R.; Jortner, J. Energy-Structure Relationships for Microscopic Solvation of Anions in Water Clusters. *J. Chem. Phys.* **1994**, *100*, 2851.
(19) Xantheas, S. S. Quantitative Description of Hydrogen Bonding in Chloride−Water Clusters. *J. Phys. Chem.* **1996**, *100*, 9703−9713.
(20) Ayotte, P.; Bailey, C. G.; Weddle, G. H.; Johnson, M. A. Vibrational Spectroscopy of Small $Br\cdot-(H_2O)_n$ and $I\cdot-(H_2O)_n$ Clusters: Infrared Characterization of the Ionic Hydrogen Bond. *J. Phys. Chem. A* **1998**, *102*, 3067.
(21) Choi, J.-H.; Kuwata, K. T.; Cao, Y.-B.; Okumura, M. Vibrational Spectroscopy of the $Cl^-(H_2O)_n$ Anionic Clusters, n = 1−5. *J. Phys. Chem. A* **1998**, *102*, 503−507.
(22) Ayotte, P.; Weddle, G. H.; Kim, J.; Kelley, J.; Johnson, M. A. A Cluster Study of Anionic Hydration: Spectroscopic Characterization of the $I\text{-}W_n$, n = 1−3, Supramolecular Complexes at the Primary Steps of Solvation. *J. Phys. Chem. A* **1999**, *103*, 443−447.
(23) Ayotte, P.; Nielsen, S. B.; Weddle, G. H.; Johnson, M. A.; Xantheas, S. S. Spectroscopic Observation of Ion-Induced Water Dimer Dissociation in the $X^-(H_2O)_2$ (X = F, Cl, Br, I) Clusters. *J. Phys. Chem. A* **1999**, *103*, 10665−10669.
(24) Dorsett, H. E.; Watts, R. O.; Xantheas, S. S. Probing Temperature Effects on the Hydrogen Bonding Network of the $Cl^-(H_2O)_2$ Cluster. *J. Phys. Chem. A* **1999**, *103*, 3351−3355.
(25) Kim, J.; Lee, H. M.; Suh, S. B.; Majumdar, D.; Kim, K. S. Comparative Ab Initio Study of the Structures, Energetics and Spectra of $X^-(H_2O)_{n=1-4}$ [X = F, Cl, Br, I] clusters. *J. Chem. Phys.* **2000**, *113*, 5259−5272.
(26) Lee, H. M.; Kim, D.; Kim, K. S. Structures, Spectra, and Electronic Properties of Halide-Water Pentamers and Hexamers, $X^-(H_2O)_{5,6}$ (X = F, Cl, Br, I): *Ab Initio* Study. *J. Chem. Phys.* **2002**, *116*, 5509.
(27) Ayala, R.; Martinez, J. M.; Pappalardo, R. R.; Marcos, E. S. Study of the Stabilization Energies of Halide-Water Clusters: An Application of First-Principles Interaction Potentials Based on a Polarizable and Flexible Model. *J. Chem. Phys.* **2004**, *121*, 7269.
(28) Kamarchik, E.; Bowman, J. M. Quantum Vibrational Analysis of Hydrated Ions Using an ab Initio Potential. *J. Phys. Chem. A* **2010**, *114*, 12945−12951.
(29) Wang, X.-G.; Carrington, T., Jr. Rovibrational Levels and Wavefunctions of $Cl^-(H_2O)$. *J. Chem. Phys.* **2014**, *140*, 204306.
(30) Kamarchik, E.; Toffoli, D.; Christiansen, O.; Bowman, J. M. Ab Initio Potential Energy and Dipole Moment Surfaces of the $F^-(H_2O)$ Complex. *Spectrochim. Acta, Part A* **2014**, *119*, 59−62.
(31) Sarka, J.; Lauvergnat, D.; Brites, V.; Császár, A. G.; Léonard, C. Rovibrational Energy Levels of the $F^-(H_2O)$ and $F^-(D_2O)$-Complexes. *Phys. Chem. Chem. Phys.* **2016**, *18*, 17678−17690.
(32) Bajaj, P.; Götz, A. W.; Paesani, F. Toward Chemical Accuracy in Description of Ion-Water Interactions through Many-Body Representations. I. Halide-Water Dimer Potential Energy Surfaces. *J. Chem. Theory Comput.* **2016**, *12*, 2698−2705.
(33) Bajaj, P.; Wang, X.-G.; Carrington, T., Jr.; Paesani, F. Vibrational Spectra of Halide-Water Dimers: Insights on Ion Hydration from Full-Dimensional Quantum Calculations on Many-Body Potential Energy Surfaces. *J. Chem. Phys.* **2018**, *148*, 102321.
(34) Bajaj, P.; Richardson, J. O.; Paesani, F. Ion-Mediated Hydrogen-Bond Rearrangement Through Tunnelling in the Iodide−Dihydrate Complex. *Nat. Chem.* **2019**, *11*, 367−374.
(35) Bajaj, P.; Riera, M.; Lin, J. K.; Medoza Montijo, Y. E.; Gazca, J.; Paesani, F. Halide Ion Microhydration: Structure, Energetics, and Spectroscopy of Small Halide−Water Clusters. *J. Phys. Chem. A* **2019**, *123*, 2843−2852.
(36) Bizzarro, B. B.; Egan, C. K.; Paesani, F. On the Nature of Halide−Water Interactions: Insights from Many-Body Representations and Density Functional Theory. *J. Chem. Theory Comput.* **2019**, *15*, 2983.
(37) Wolke, C. T.; Menges, F. S.; Tötsch, N.; Gorlova, O.; Fournier, J. A.; Weddle, G. H.; Johnson, M. A.; Heine, N.; Esser, T. K.; Knorke, H.; et al. Thermodynamics of Water Dimer Dissociation in the Primary Hydration Shell of the Iodide Ion with Temperature-Dependent Vibrational Predissociation Spectroscopy. *J. Phys. Chem. A* **2015**, *119*, 1859−1866.
(38) Yang, N.; Duong, C. H.; Kelleher, P. J.; Johnson, M. A.; McCoy, A. B. Isolation of Site-Specific Anharmonicities of Individual Water Molecules in the $I^-(H_2O)_2$ Complex Using Tag-Free, Isotopomer Selective IR-IR Double Resonance. *Chem. Phys. Lett.* **2017**, *690*, 159−171.
(39) Ma, X.; Yang, N.; Johnson, M. A.; Hase, W. J. Anharmonic Densities of States for Vibrationally Excited $I^-(H_2O)$, $(H_2O)_2$, and $I^-(H_2O)_2$. *J. Chem. Theory Comput.* **2018**, *14*, 3986−3997.
(40) Yang, N.; Duong, C. H.; Kelleher, P. J.; Johnson, M. A. Unmasking Rare, Large-Amplitude Motions in D_2-Tagged $I^-(H_2O)_2$ Isotopomers with Two-Color, Infrared-Infrared Vibrational Predissociation Spectroscopy. *J. Phys. Chem. Lett.* **2018**, *9*, 3744−3750.
(41) Cheng, X.; Steele, R. P. Efficient Anharmonic Vibrational Spectroscopy for Large Molecules Using Local-Mode Coordinates. *J. Chem. Phys.* **2014**, *141*, 104105.
(42) Cheng, X.; Talbot, J. J.; Steele, R. P. Tuning Vibrational Mode Localization with Frequency Windowing. *J. Chem. Phys.* **2016**, *145*, 124112.
(43) Wang, Y.; Bowman, J. M. *Ab Initio* Potential and Dipole Moment Surfaces for Water. II. Local-Monomer Calculations of the Infrared Spectra of Water Clusters. *J. Chem. Phys.* **2011**, *134*, 154510.
(44) Ayotte, P.; Weddle, G. H.; Kim, J.; Johnson, M. A. Mass-Selected "Matrix Isolation" Infrared Spectroscopy of the $I^-(H_2O)_2$ Complex: Making and Breaking the Inter-Water Hydrogen-Bond. *Chem. Phys.* **1998**, *239*, 485−491.
(45) Richardson, J. O.; Althorpe, S. C. Ring-Polymer Instanton Method for Calculating Tunneling Splittings. *J. Chem. Phys.* **2011**, *134*, 054109.
(46) Richardson, J. O.; Althorpe, S. C.; Wales, D. J. Instanton Calculations of Tunneling Splittings for Water Dimer and Trimer. *J. Chem. Phys.* **2011**, *135*, 124109.
(47) Bakker, H.; Kropman, M.; Omta, A. Effect of Ions on the Structure and Dynamics of Liquid Water. *J. Phys.: Condens. Matter* **2005**, *17*, S3215.
(48) Laage, D.; Hynes, J. T. Reorientational Dynamics of Water Molecules in Anionic Hydration Shells. *Proc. Natl. Acad. Sci. U. S. A.* **2007**, *104*, 11167−11172.
(49) Stirnemann, G.; Wernerson, E.; Jungwirth, P.; Laage, D. Mechanisms of Acceleration and Retardation of Water Dynamics by Ions. *J. Am. Chem. Soc.* **2013**, *135*, 11824−11831.

DOI: 10.1021/acs.jpclett.9b00899
J. Phys. Chem. Lett. 2019, 10, 2823−2828